Original Study **Open Access**

Dorota Pawlus*

The Temperature Field Effect on Dynamic Stability Response of Three-layered Annular Plates for Different Ratios of Imperfection

https://doi.org/10.2478/sgem-2023-0005
received September 20, 2022; accepted January 5, 2023.

Abstract: The paper presents the temperature field effect on the dynamic stability problem of plates with imperfection. The main objective is to conduct numerical investigations which show the relations between the imperfection ratio and plate dynamic response in a thermal environment. The plate is composed of three layers: thin facings and a thicker core. The plate can be loaded mechanically and thermally or only thermally. The facings are mechanically compressed with the forces acting in a plane. The temperature field model is defined by the temperature difference, which occurs between the plate edges. Two plate models are examined as follows: built using the approximation methods – orthogonalization and finite differences – and composed of finite elements. The analytical and numerical solution procedure is the main one, which is the proposal to perform the problem analysis. The plate reaction is described by the obtained values of the critical temperature differences for plates loaded only thermally and by the critical mechanical loads and the corresponding temperature differences for plates loaded mechanically and subjected to the uncoupled temperature field. The effect of the plate imperfection ratio under time-dependent loads is shown by numerous observations and results, which are shown graphically. The importance of the imperfection ratio on the plate's dynamic stability response in complex loading conditions is studied.

Keywords: three-layered annular plate; dynamic stability; imperfection; thermal loading; finite difference method; finite element method.

***Corresponding author: Dorota Pawlus,** Faculty of Mechanical Engineering and Computer Science, University of Bielsko-Biala Willowa 2, 43-309 Bielsko-Biala, Poland, E-mail: doro@ath.bielsko.pl

1 Introduction

The effect of the dynamic response of the composite plate depends on various parameters. These include the imperfection ratios whose values determine the predeflection shape of the plate. A plate subjected to mechanical and thermal loads increasing in time formulates a time-dependent complex problem, whose results are strongly related to the plate geometrical parameters. The annular and circular composite plates, which can be used in different kinds of industries, such as mechanical, civil engineering, and aerospace, can be subjected to the complex work conditions. This is the reason that the thermomechanical evaluation of plate sensitivity is still a current issue addressed in numerous works. Few works strictly focus on the issue of the imperfection of composite annular plates. Selected papers concerning the issue of buckling of mechanically or/and thermally loaded plates where the plate geometry has been taken into account are presented in the literature review.

The general solution and dynamic behavior of sandwich annular and circular plates are presented in works [1] and [2]. The thermal buckling effect of moderately thick functionally graded material (FGM) annular plate is presented in paper [3]. The thermoelastic problem showing the reactions of the imperfect, radially graded annular plate with a heated edge is presented in work [4]. The effect of temperature on the buckling behavior of the annular plate is presented in papers [5–7]. The elements of the critical state, like critical temperature and the corresponding modes, are examined for different materials and geometrical plate parameters. The FGM annular plates with imperfections are presented in paper [8]. Both buckling and dynamic postbuckling reactions are the main problems of consideration. The thermomechanical buckling of perforated, functionally graded annular sector plates under uniform temperature rises and radial, circumferential, or biaxial mechanical

loads is investigated in work [9]. The final results present the effect of the sector geometry, direction of the mechanical loads, and the combination of the thermal and mechanical loads on the buckling loads and mode shapes. The viscoelastic FGM annular plates with different geometrical, material, and load parameters are presented in work [10]. The paper presents the unified dynamic analysis method for a viscoelastic FGM annular plate.

The novelties presented in this paper concern the numerical investigations which are focused on the evaluation of the reactions of the composite plate to the action of the temperature field or the participation of the temperature field in complex thermomechanical loading. The imperfection of the shape geometry of the plate's initial surface is the main analyzed element, which changes the dynamic response of the plate. The effect of various geometrical imperfect forms of the plate surface predeflection has been examined: waved circumferential predeflection, which corresponds to the plate buckling mode, complex initial shape, which is composed of rotational axisymmetrical predeflection, and the circumferential waved form for positive or mixed positive and negative numbers, which calibrate the grade of plate predeflection. The participation of various imperfections of the plate surface, which initiate the dynamic buckling phenomenon, complements the existing analyses and significantly enriches the cognition of the examined layered structure of the plate showing its resistance to the shape imperfections. The presented exemplary results of the numerous numerical analyses create both a practically important and scientifically interesting image of the buckling sensitivity of the structures to existing imperfections. Some numerical results are presented in work [11]. The additional and wider observations, numerical calculations, and results shown in the figures and the tables presented in this work make recognition of the formulated problem richer. To the best of the author's knowledge, the so-formulated thermomechanical problem and the idea to observe the plate buckling sensitivity on variously defined imperfections have not been sufficiently considered.

The method of the analytical and numerical solution to the problem as proposed in this paper refers to the solution of mechanically loaded annular plate presented in works [12], [13], [14]. The imperfection issue is analyzed in work [14] and particularly in work [15] for plates that are only loaded mechanically. Thermal and thermomechanical problems are examined for a layered, composite plate in work [16], [17]. The observations for a composite three-layered plate with a core layer made of viscoelastic material are presented in [18].

2 Problem Formulation

The three-layered annular plate composed of thin steel facings and a thicker foam core is the object of consideration. The plate cross section is symmetric. The analyzed forms of plate buckling can be axisymmetrical or asymmetrical. The plate is subjected to a complex thermomechanical state of loading. It is mechanically loaded by the compressing forces linearly increasing in time, which are uniformly distributed on the outer facings. The temperature field surrounds the plate's inner and outer perimeters. The temperature difference between the inner and outer plate edges creates the thermal gradient. The temperature difference can be fixed, constant in time, or it can change, dynamically increasing in time. Three models of loading, showing the temperature field effect on the dynamic plate reaction, are acceptable: thermal loading with the temperature difference between the plate edges increasing in time, both mechanical and thermal loading with mechanical and thermal loads increasing in time, and mechanical loading increasing in time, which is connected to the constant in time action of the temperature field. It should be emphasized that thermal loading is defined by the uncoupled temperature field, whose parameters are arbitrarily assumed.

The equations (1) and (2) express the thermomechanical loading quickly increasing in time:

$$p = st \tag{1}$$

$$\Delta T = at \tag{2}$$

where p is the mechanical stress, s the rate of the mechanical loading growth, ΔT the temperature difference between plate edges, a the rate of the temperature loading growth, and t is the time.

The plate is loaded mechanically with the compressive forces uniformly distributed on the outer perimeter of the facings. The action of the outer forces on the lateral surfaces of both plate facings determines the compressive mechanical stress p. The plate model is presented in Figure 1. The plate is located in a temperature field with different values of temperatures T_i and T_o in the plate's inner hole and area of the outer perimeter, respectively. Both plate edges are slidably clamped. Two cases of thermal gradients are considered: positive where temperature T_i in the plate's hole is higher than in the outer surroundings ($T_i > T_o$) and negative where the temperature values are opposite ($T_i < T_o$).

The main assumptions which are adopted to describe the thermal environment are as follows:

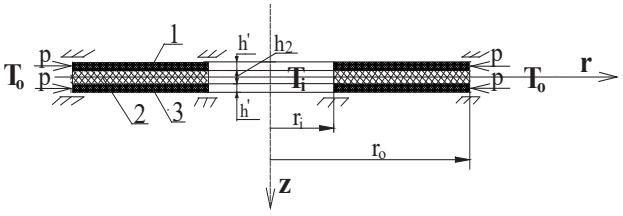

Figure 1: Scheme of thermomechanical loading of a three-layered annular plate built of outer layers 1 and 3 and middle layer 2.

- axisymmetric and flat temperature field,
- the lack of heat exchange between the plate surfaces,
- the heat flow is only in a radial direction of the plate facings (see Eq. (3)), and
- the material parameters are fixed and do not depend on temperature changes.

To express the parameters of the dynamic critical state of the plate, the criterion of the loss of plate stability was assumed. According to the criterion presented by Wolmir [19], the plate loses its stability at the moment when the first maximum value of deflection velocity is observed for the point with the maximum deflection.

3 Problem Solution

The main method of solution is based on an analytical and numerical analysis which uses the following approximation methods: orthogonalization and finite difference (the Finite Difference Model – FDM plate). The influence of various ratios of imperfections on plate stability response is expressed by the elements of assumed equation (9), which determine the shapes of plate predeflection. Equation (9) is composed of two terms: axisymmetrical and a term dependent on the number of circumferential waves. Assumed calibrating numbers change the participation of the mentioned two terms and make it possible to produce various forms of plate predeflection. The solution procedure is presented in the works [12,13,14,17] in detail.

Additionally, the finite element method has been used to evaluate selected examples of the plates being examined (the Finite Element Method - FEM plate). The ABAQUS system was used to conduct the calculations.

3.1 Solution Procedure Using the Finite Difference Method

The main elements of the solution procedure are as follows: formulation of the system of the dynamic equilibrium equations of each plate layer, description of the transversally symmetrical deformation of the three-layered structure, formulation of the equations for angles describing the broken line in the plate cross section for the core layer in radial and circumferential directions, usage of the linear physical relation in the plate facings and the core, formulation of the sectional forces and moments in facings including the thermal elements, and determination of the resultant membrane forces including the assumed stress function.

The temperature distribution in the radial direction of the plate facings is expressed by the logarithmic equation [20]

$$T_N = T_o + \frac{T_i - T_o}{\ln \rho_i} \ln \rho \tag{3}$$

where T_i and T_o are the temperatures of the inner and outer plate perimeters, respectively (see Fig. 1), $\rho = \frac{r}{r_o}$ the dimensionless plate radius, $\rho_i = \frac{r_i}{r_o}$ the dimensionless inner plate radius, and r_o is the outer plate radius.

The basic equation describing the plate deflections in the dynamic problem takes the following form:

$$\begin{aligned} &k_1 w_{d',rrrr} + \frac{2k_1}{r} w_{d',rrr} - \frac{k_1}{r^2} w_{d',rr} + \frac{k_1}{r^3} w_{d',r} + \frac{k_1}{r^4} w_{d',\theta\theta\theta\theta} + \frac{2(k_1+k_2)}{r^4} w_{d',\theta\theta} + \\ &+ \frac{2k_2}{r^2} w_{d',rr\theta\theta} - \frac{2k_2}{r^3} w_{d',r\theta\theta} - G_2 \frac{H'}{h_2} \frac{1}{r} \left(\gamma_{,\theta} + \delta + r\delta_{,r} + H' \frac{1}{r} w_{d',\theta\theta} + H' w_{d',r} + H' r w_{d',rr} \right) \\ &= \frac{2h'}{r} \left(\frac{2}{r^2} \Phi_{,\theta} w_{,r\theta} - \frac{2}{r} \Phi_{,r\theta} w_{,r\theta} + \frac{2}{r^2} w_{,\theta} \Phi_{,r\theta} - \frac{2}{r^3} w_{,\theta} \Phi_{,\theta} + w_{,r} \Phi_{,rr} + \Phi_{,r} w_{,rr} + \right. \\ &\left. + \frac{1}{r} \Phi_{,\theta\theta} w_{,rr} + \frac{1}{r} \Phi_{,rr} w_{,\theta\theta} \right) - \mathrm{M} w_{\mathrm{d'tt}} \end{aligned} \tag{4}$$

where w_d is the additional plate deflection, $k_1 = 2D$, $k_2 = 4D_{r\theta} + \nu k_1$; $D = \frac{Eh^3}{12(1-\nu^2)}$ is the plate rigidity; $D_{r\theta} = \frac{Gh^3}{12}$ is flexural rigidity of the facings; E and ν are the Young's modulus and Poisson's ratio of the facing material, respectively; h is the total plate thickness; δ and γ are the differences of radial and circumferential displacements of the points, respectively, in the middle surfaces of the facings $\delta = u_3 - u_1$, $\gamma = v_3 - v_1$; $H' = h' + h_2$; Φ is the stress function; w is the plate total deflection; $M = 2h'\mu + h_2\mu_2$; μ and μ_2 are the facing and core mass density, respectively; h' is the facings' thickness and h_2 is the core thickness.

Equation (4) has been obtained after adding the summands of the dynamic equilibrium equations of forces in the transversal plate direction, which have been derived for each plate layer: the facings and the core. Then, the relations for the resultant radial and circumferential

forces and the resultant membrane forces expressed by the introduced stress function Φ have been inserted.

The boundary conditions for the plate slidably clamped on both edges are as follows:

$$w\big|_{r=r_i(r_o)}=0,\ w_r\big|_{r=r_i(r_o)}=0,\ \delta=\gamma\big|_{r=r_i(r_o)}=0,\ \delta_r\big|_{r=r_i(r_o)}=0 \tag{5}$$

The initial and loading conditions are as follows:

$$w_d\big|_{t=0}=0,\ w_{d,t}\big|_{t=0}=0 \tag{6}$$

The conditions associated with the mechanically loaded plate edges are the following:

$$\sigma_r\big|_{r=r_i}=-p(t)d_1,\ \sigma_r\big|_{r=r_o}=-p(t)d_2,\ \tau_{r\theta}\big|_{r=r_i(r_o)}=0, \tag{7}$$

where σ_r is the radial stress, $\tau_{r\theta}$ the shear stress, and d_1, d_2 are the quantities equal to 0 or 1, determining the loading of the inner or/and outer plate perimeter.

Conditions for the plate edges subjected to only thermal loads are expressed by the equation

$$\sigma_r\big|_{r=r_i}=0,\quad \sigma_r\big|_{r=r_o}=0 \tag{8}$$

The form of plate imperfection ζ_o ($\zeta_o = w_o/h$), important in the presented analysis, is expressed by the following equation presented in [21]:

$$\zeta_o(\rho,\theta)=\xi_1(\rho)\eta(\rho)+\xi_2(\rho)\eta(\rho)\cos(m\theta) \tag{9}$$

where w_o is the plate initial deflection, m the number of initial circumferential waves, ξ_1, ξ_2 are the calibrating numbers, $\eta(\rho)$ is a function: $\eta(\rho)=\rho^4+A_1\rho^2+A_2\rho^2 ln r+A_3 ln\rho+A_4$, A_i are the quantities fulfilling the conditions of clamped edges.

The solution is based on shape functions for the additional plate deflection ζ_1 [21]

$$\zeta_1(\rho,\theta,t)=X_1(\rho,t)\cos(m\theta), \tag{10}$$

stress function F [21]

$$F(\rho,\theta,t)=F_a(\rho,t)+F_b(\rho,t)\cos(m\theta)+F_c(\rho,t)\cos(2m\theta), \tag{11}$$

and differences $\bar{\delta}$, $\bar{\gamma}$ [14]:

$$\bar{\delta}(\rho,\theta,t)=\bar{\delta}(\rho,t)\cos(m\theta),\ \bar{\gamma}(\rho,\theta,t)=\bar{\gamma}(\rho,t)\sin(m\theta) \tag{12}$$

where $\zeta_1=\frac{w_d}{h}$, $F=\frac{\Phi}{Eh^2}$, $\bar{\delta}=\frac{\delta}{h}$, $\bar{\gamma}=\frac{\gamma}{h}$, m are the number of circumferential waves, which is compatible with the initial number (see Eq. (9)) and characterizes the form of plate buckling – the mode for plates with ξ_1 calibrating number equal to $\xi_1 = 0$.

Using the orthogonalization method after elimination of the angular variable θ and approximation of the derivatives with respect to ρ by the central differences in the discrete points, the basic system of differential equations has been established:

$$\boldsymbol{PU}+\boldsymbol{Q}=\ddot{\boldsymbol{U}}_{\boldsymbol{K}} \tag{13}$$

$$\boldsymbol{M}_Y\boldsymbol{Y}=\boldsymbol{Q}_{Y\Delta T} \tag{14}$$

$$\boldsymbol{M}_V\boldsymbol{V}=\boldsymbol{Q}_V \tag{15}$$

$$\boldsymbol{M}_Z\boldsymbol{Z}=\boldsymbol{Q}_Z \tag{16}$$

$$\boldsymbol{M}_D\boldsymbol{D}+\boldsymbol{M}_U\boldsymbol{U}+\boldsymbol{M}_G\boldsymbol{G}=0 \tag{17}$$

$$\boldsymbol{M}_{GG}\boldsymbol{G}+\boldsymbol{M}_{GU}\boldsymbol{U}+\boldsymbol{M}_{GD}\boldsymbol{D}=0 \tag{18}$$

For a mechanically loaded plate with a constant in time–temperature difference $\Delta T = T_i - T_o$ between the edges, Eq. (14) has been modified to the form

$$\boldsymbol{M}_Y\boldsymbol{Y}=\boldsymbol{Q}_{Y\Delta T const} \tag{19}$$

where $\boldsymbol{U},\boldsymbol{Y},\boldsymbol{Z},\boldsymbol{V}$ are the vectors whose elements consist of the additional deflections and components of the stress function, respectively; $\ddot{\boldsymbol{U}}_{\boldsymbol{K}}$ is a vector whose elements are expressed by the products of the derivative of the additional deflection with respect to time t and number K, equal to $K=TK7^2\cdot\frac{h'}{h}\cdot r_o h_2 M$; $\boldsymbol{Q},\boldsymbol{Q}_V,\boldsymbol{Q}_Y,\boldsymbol{Q}_z,\boldsymbol{D},\boldsymbol{G}$ are the vectors whose elements consist of the plate material parameters, geometrical dimensions, initial and additional deflections, number m, dimension radius ρ, and displacement differences δ; γ; $\boldsymbol{Q}_{Y\Delta T}$ is a vector whose elements are expressed as the difference between the suitable element of vector $\boldsymbol{Q}_Y$ (vector $\boldsymbol{Q}_Y$ is used for plates which are not subjected to the temperature field) and the number $\rho\cdot S\cdot T_{N'\rho}$, which differs in time, $S=\frac{r_z^2}{h^2}\alpha$; $\boldsymbol{Q}_{Y\Delta T const}$ is a vector whose elements are expressed as the difference between the suitable element of vector $\boldsymbol{Q}_Y$

Table 1: Parameters of the plate model.

Geometrical parameters			
Inner radius r_i, m	0.2		
Outer radius r_o, m	0.5		
Facing thickness h', mm	1		
Core thickness h_2, mm	5		
Ratio of plate initial deflection ξ_2	0.5, 1, 2		
Material parameters			
Steel facing		Polyurethane foam of core	
Young's modulus E, GPa	210	E_2, MPa	13
Kirchhoff's modulus G, GPa	80	G_2, MPa	5
Poisson's ratio ν	0.3	ν_2	0.3
Mass density μ, kg/m³	7850	μ_2, kg/m³	64
Linear expansion coefficient a, 1/K	1.2×10^{-5}	a_2, 1/K	7×10^{-5}
Loading parameters			
Rate of thermal loading growth a, K/s (TK7, 1/s)	200 (20), 800 (20)		
Rate of mechanical loading growth s, MPa/s (K7, 1/s)	931 (20)		
Constant temperature difference ΔT, K	800		

and the number $S\frac{T_i - T_o}{\ln\rho_i}$, which is constant in time; and $\boldsymbol{M}_Y, \boldsymbol{M}_V, \boldsymbol{M}_Z, \boldsymbol{M}_D, \boldsymbol{M}_G, \boldsymbol{M}_U, \boldsymbol{M}_{GG}, \boldsymbol{M}_{GD}, \boldsymbol{P}, \boldsymbol{M}_{GU}$ are the matrices whose elements consist of the plate material parameters, geometrical dimensions, number m, FDM parameter b (b – the interval in the finite difference method), and dimension radius ρ.

The Runge–Kutta's integration method for the initial state of the plate has been used in the solution of the presented system of equations.

The dimensionless time connected with mechanical loading (see Equation (1)) is expressed by $t^*=t\times K7$, where $K7$ is the number expressing the rate of mechanical loading growth but connected with thermal loading (see Equation (2)) and is expressed as $t^*=t\times TK7$, where $TK7$ is the number expressing the rate of thermal loading growth.

3.2 Method of Solution Using the Finite Element Method

The plate model built with the use of the finite element method has been calculated in the ABAQUS system. The calculations were carried out at the Academic Computer Center CYFRONET-CRACOW (KBN/SGI_ORIGIN_2000/PLodzka/030/1999). The dynamic module is the main option, which was applied in the dynamic solution procedure [22]. The three-layered structure of the FEM plate model is composed of shell elements and solid ones to build the meshes of the plate facings and the core, respectively. 3D nine-node shell elements with six active degrees of freedom and 3D 27-node solid elements with three active degrees of freedom were used. The surface contact interaction with the TIE option was assumed to connect the surfaces of the facings and the core meshes.

4 Exemplary Results and Discussion

Table 1 presents the assumed material, geometrical, and loading parameters of the examined plate models.

The ratio ξ_2 of plate initial deflection is described in figures as *ksi*2. In the present analysis, the polyurethane foam of the core material is treated as elastic and isotropic. The rheological properties of this material are not taken into account. The viscoelastic parameters of foam material have been assumed in investigations presented by Pawlus in works [14] and [18] concerning the three-layered annular plates under lateral dynamic mechanical load as well as thermal load. The plate is loaded on the outer edge with

the rate s. The plate is subjected to a thermal field with a positive or negative gradient.

Two main models of plate loading are analyzed: a plate thermally loaded and a plate mechanically and thermally loaded. The critical dynamic temperature difference ΔT_{crdyn} is the main calculation result for plates loaded only thermally. Critical dynamic mechanical load p_{crdyn} is the main result of the calculations of plates loaded mechanically and thermally. Additionally, to recognize the plate dynamic behavior, the time histories of plate deflections and the velocity of deflections are designed. The analyzed problem is the multiparameter task, for which the ratio of plate predeflection is the basic variable.

4.1 Convergence Analysis for the FDM Plate Model

The first step of numerical analysis, which is performed with using the finite difference method, is the choice of the number N of discrete points. Tables 1 and 2 present the results of the critical dynamic temperature ΔT_{crdyn} and the critical dynamic load p_{crdyn} with relative temperature ΔT_b for the FDM plate model with a different number N of discrete points equal to N = 11, 14, 17, 21, 26. Table 2 presents the critical dynamic temperature differences ΔT_{crdyn} of the FDM plate model with the imperfection ratio ξ_2 = 0.5. The plate is thermally loaded with a positive temperature gradient. Values of ΔT_{crdyn} show a tendency to increase with the number N of discrete points. Also, the relative difference between the values of ΔT_{crdyn} for number N = 26 and 21 increases with the number m. Its value for the minimal value of ΔT_{crdyn}, which exists for m = 7, is less than 5%, which is treated as a technical error. This is the way the number N = 14 of the discrete points has been chosen in the FDM numerical calculations. Table 3 presents the critical dynamic mechanical load p_{crdyn} and corresponding temperature differences ΔT_b for the axisymmetric (m = 0) FDM plate model with the imperfection ratio ξ_2 = 2 loaded mechanically and located in the thermal environment. The temperature field model is characterized by the rate a of a temperature linear growth equal to a = 800 K/s and a positive temperature gradient. The values of critical load p_{crdyn} are comparable to the relative difference between the values calculated for a different number N, which is about 5% of the technical error.

In summary, it can be noticed that values of the critical temperature difference and the critical load are converged. It confirms that the solution process is correct and the numerical calculations are accurate.

Table 2: The values of the dynamic, critical temperature differences ΔT_{crdyn} depending on the number N of discrete points for the FDM plate model with the imperfection ratio ξ_2 = 0.5 subjected to a positive gradient of the temperature field.

m	ΔT_{crdyn} (K)				
	N = 11	N = 14	N = 17	N = 21	N = 26
0	128.6	130.0	130.1	131.6	131.5
1	131.9	133.7	133.7	134.2	134.7
2	133.5	135.5	135.5	137.2	137.0
3	126.4	129.3	131.2	130.9	132.4
4	117.5	120.7	122.1	123.5	124.8
5	108.7	112.3	114.9	115.9	117.1
6	105.7	108.9	110.4	112.8	113.8
7	103.8	106.8	108.8	109.5	111.7
8	103.7	107.9	110.3	112.8	116.4

4.2 Thermally Loaded Plate

Figures 2 and 3 show a comparison of the thermal reaction of two FDM plate models: axisymmetrical m = 0 and circumferentially waved m = 7. Number m = 7 of plate buckling waves in a circumferential direction corresponds to the minimal value of the critical temperature difference between the plate edges ΔT_{crdyn} (see Table 2). The plate models are loaded thermally with the rate of loading growth a = 200 K/s and a = 800 K/s. A temperature field model with a positive gradient is considered. Figures 2 and 3 show the strong plate reaction on the temperature growth with a high value of the rate a, a = 800 K/s. Then, both the plate modes m = 0 and m = 7 lose dynamic stability quickly. However, the temperature difference, which exists

Table 3: The values of the dynamic, critical mechanical loads p_{crdyn} with the corresponding temperature differences ΔT_b for the axisymmetric FDM plate model (m = 0) with the imperfection ratio ξ_2 = 2 subjected to a mechanical load and increasing with the value a = 800 K/s temperature field with a positive gradient.

Number N	11	14	17	21	26
p_{crdyn} (MPa)/ΔT_b (K)	30.74/26.4	29.35/25.2	31.21/26.8	30.74/26.4	31.21/26.8

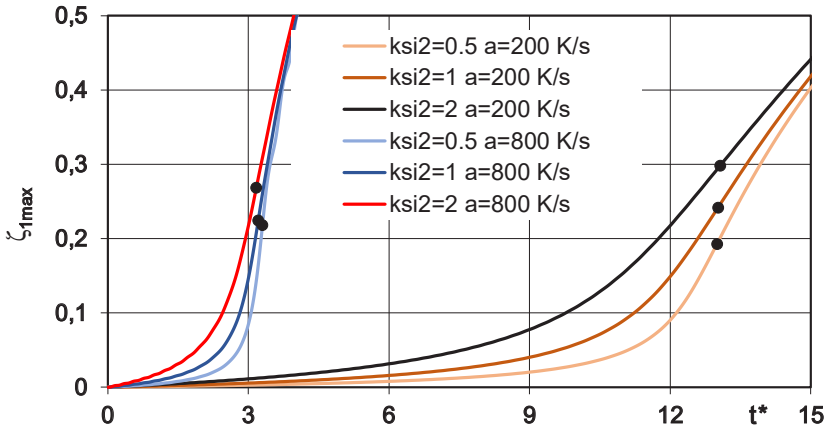

Figure 2: Deflections of the axisymmetrical $m = 0$ plate model versus imperfection ratio ξ_2 under a temperature field with a positive gradient and two rates $a = 200$ K/s and $a = 800$ K/s.

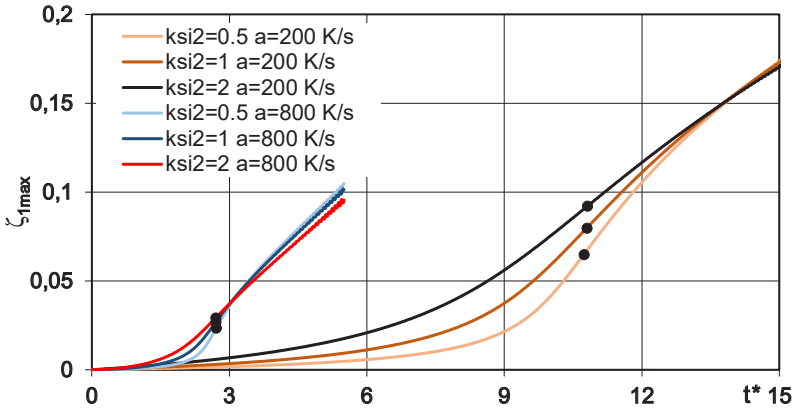

Figure 3: Deflections of the asymmetrical $m = 7$ plate model versus the imperfection ratio ξ_2 under a temperature field with a positive gradient and two rates $a = 200$ K/s and $a = 800$ K/s.

Table 4: Values of critical temperature differences ΔT_{crdyn} for the axisymmetrical $m = 0$ FDM plate model versus the imperfection ratio ξ_2 under a temperature field with a positive gradient and two rates $a = 200$ K/s and $a = 800$ K/s.

Rate a (K/s)	ΔT_{crdyn} (K)		
	ξ_2		
	0.5	**1**	**2**
200	130.0	130.2	130.7
800	132.0	128.4	126.8

Table 5: Values of critical temperature differences ΔT_{crdyn} for the asymmetrical $m = 7$ FDM plate model versus the imperfection rate ξ_2 under a temperature field with a positive gradient and two rates $a = 200$ K/s and $a = 800$ K/s.

Ratio a (K/s)	ΔT_{crdyn} (K)		
	ξ_2		
	0.5	**1**	**2**
200	107.4	108.0	108.2
800	108.8	108.4	108.4

between the plate edges at the critical buckling moment for the two examined rates a, and the imperfection ratios ξ_2 do not differ significantly. Tables 4 and 5 present the values of the critical temperature differences ΔT_{crdyn} for two FDM plate models $m = 0$ and $m = 7$, respectively. The values of ΔT_{crdyn} for the waved $m = 7$ plate model are smaller than those observed for the axisymmetrical $m = 0$ one. It shows that a full analysis, which includes the asymmetric plate modes, is required to recognize the different plate thermal reactions. Imperfection ratios do not have a significant meaning here.

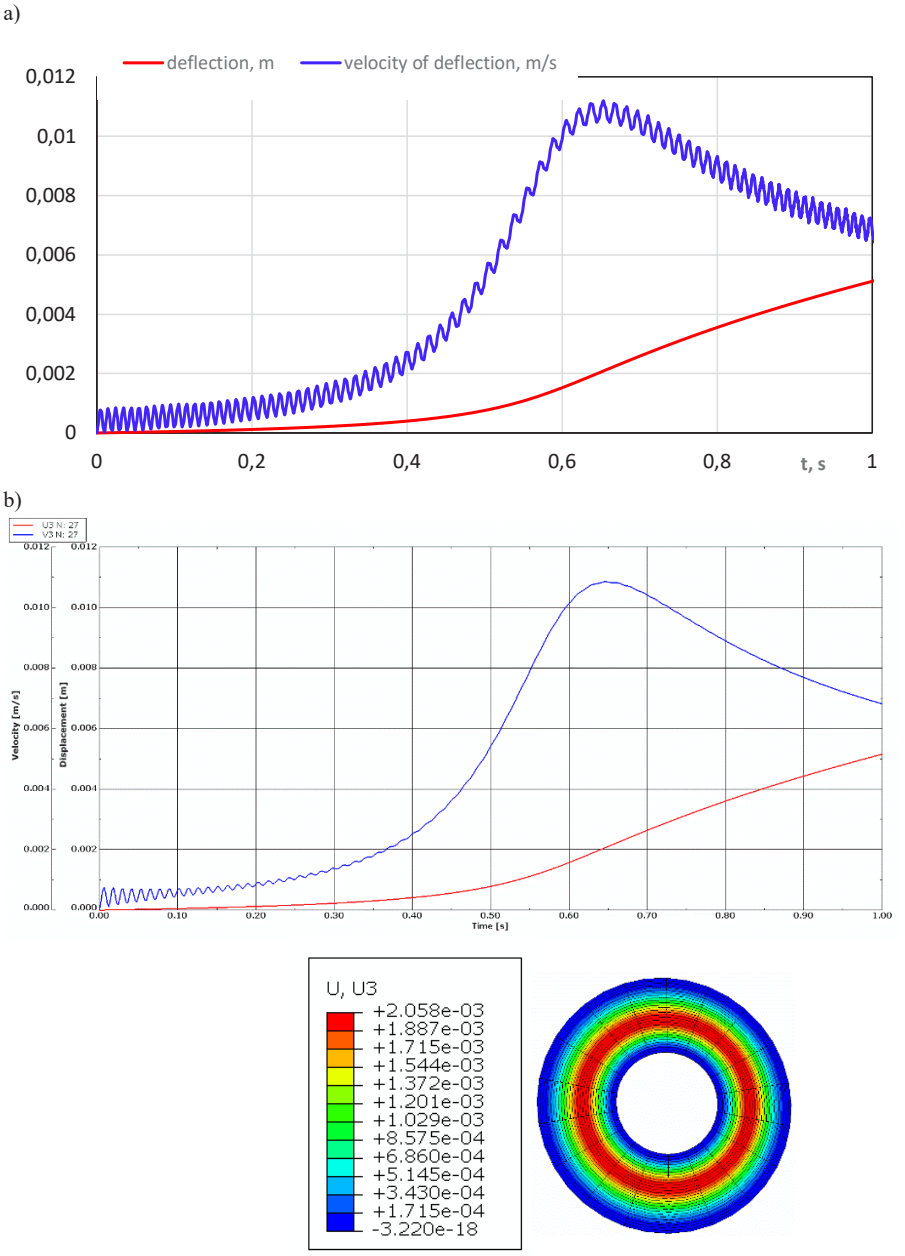

Figure 4: Time histories of deflections and velocity of deflection for plate model $m = 0$ with the imperfection ratio $\xi_2 = 2$ loaded thermally with a positive temperature gradient, with rate $a = 200$ K/s: a) FDM model, b) FEM model with critical deflection form.

Table 6: Values of critical temperature differences ΔT_{crdyn} for the axisymmetrical $m = 0$ FEM plate model versus the imperfection ratio ξ_2 under a temperature field with a positive gradient and two rates $a = 200$ K/s and $a = 800$ K/s.

Rate a (K/s)	ΔT_{crdyn} **(K)**		
	ξ_2		
	0.5	**1**	**2**
200	115.2	121.2	129.2
800	124.8	128.0	132.8

Exemplary time histories of plate deflection and velocity of deflection for the FDM and FEM plate models are shown in Figure 4. Additionally, the axisymmetric $m = 0$ form of plate buckling is shown (see Fig. 4b). The FEM results are for the plate with the imperfection ratio $\xi_2 = 2$ loaded thermally with $a = 200$ K/s. On comparing the results shown in Fig. 4a and b, a good compatibility of responses of the FDM and FEM plate models is observed. Table 6 presents the values of the critical temperature differences ΔT_{crdyn} for the axisymmetric $m = 0$ FEM plate

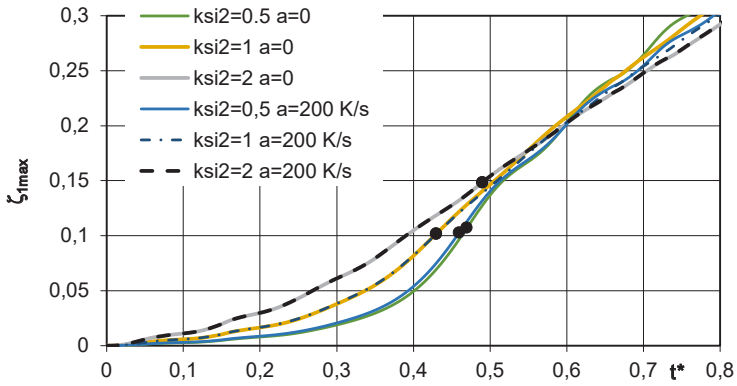

Figure 5: Deflections of the asymmetrical $m = 7$ plate model with different imperfection ratios ξ_2 under mechanical load and thermal load with a positive temperature gradient and various rates a.

Table 7: Values of critical dynamic mechanical loads p_{crdyn} and corresponding temperature differences ΔT_b for the axisymmetrical $m = 0$ FDM plate model thermomechanically loaded and imperfected with ratio $\xi_2 = 2$.

a (K/s) ΔT (K)	p_{crdyn} (MPa)/DT_b (K)	
	$\xi_2 = 2$	
	Positive gradient	**Negative gradient**
0	35.8/0	35.8/0
200	34.47/7.4	37.26/8.0
800	27.12/23.2	42.39/36.4
$\Delta T = 800$	22.36/19.2	44.25/38.0

model loaded with two rates $a = 200$ K/s and $a = 800$ K/s. The differences between the critical values ΔT_{crdyn} for the FEM plate model are clearer than for the FDM plate mode. With an increase in imperfection ratio ξ_2 and temperature growth rate a, loss of dynamic stability occurs for a higher value of the temperature field.

In summary, it can be observed that the analyzed plate modes $m = 0$ and $m = 7$ and plate cases loaded with different rates a influence the values of the critical temperature differences. The imperfection ratio ξ_2 for the asymmetric ($m = 7$) plate mode does not have a significant effect on the critical temperature difference ΔT_{crdyn}.

4.3 Mechanically and Thermally Loaded Plate

The two plate modes $m = 0$ and $m = 7$ present the plate reaction on the action of the mechanical load and temperature field. The selected modes enable showing the behavior of the axisymmetric $m = 0$ and asymmetric plates $m = 7$, whose value of the critical load is minimal [12–14]. Both thermomechanical responses of the FDM and FEM plate modes are shown in Figs 5–9. Plate imperfection is expressed by the ratio $\xi_1 = 0$ and various values of the ratio ξ_2 (see Eq. (9)). The plates are compressed on the outer edge with a growth rate equal to $s = 931$ MPa/s ($K7 = 20$ 1/s).

Figure 5 shows the effect of the imperfection ratio ξ_2 and thermal loading growth a. The presented results are for the asymmetric $m = 7$ FDM plate mode. The analyzed value of the temperature loading growth a does not change the dynamic response of the plate subjected to only the mechanical load $a = 0$. Very small differences are observed for a plate with the value $\xi_2 = 0.5$.

A comparison between the reactions of plate modes $m = 0$ and $m = 7$ is shown in Fig. 6. Plates with the imperfection ratio $\xi_2 = 2$ are subjected to three models of thermomechanical loads: without temperature field $a = 0$, with increasing in time temperature difference between the plate edges $a = 200$ K/s and $a = 800$ K/s, and the model with a fixed value of the temperature field $\Delta T = 800$ K (marked in the figures as DT). The results presented for a greater value of the rate $a = 800$ K/s or for the plate located in a thermal environment with a high, constant temperature difference equal to $\Delta T = 800$ K can be the exemplary dynamic response of the plate under the impact of thermal loading, which exists during the aerodynamic or laser heating mentioned in work [8]. Additionally, two temperature gradients are taken into account: positive with a higher value of temperature on the inner plate edge and negative with a higher value of temperature on the outer edge. Plate mode $m = 0$ responds differently to temperature field profiles. The detailed values are presented in Table 7. Critical dynamic load p_{crdyn} and the corresponding temperature difference ΔT_b, when a loss of plate stability occurs, decrease with the growth of the rate a for a temperature field with a positive gradient

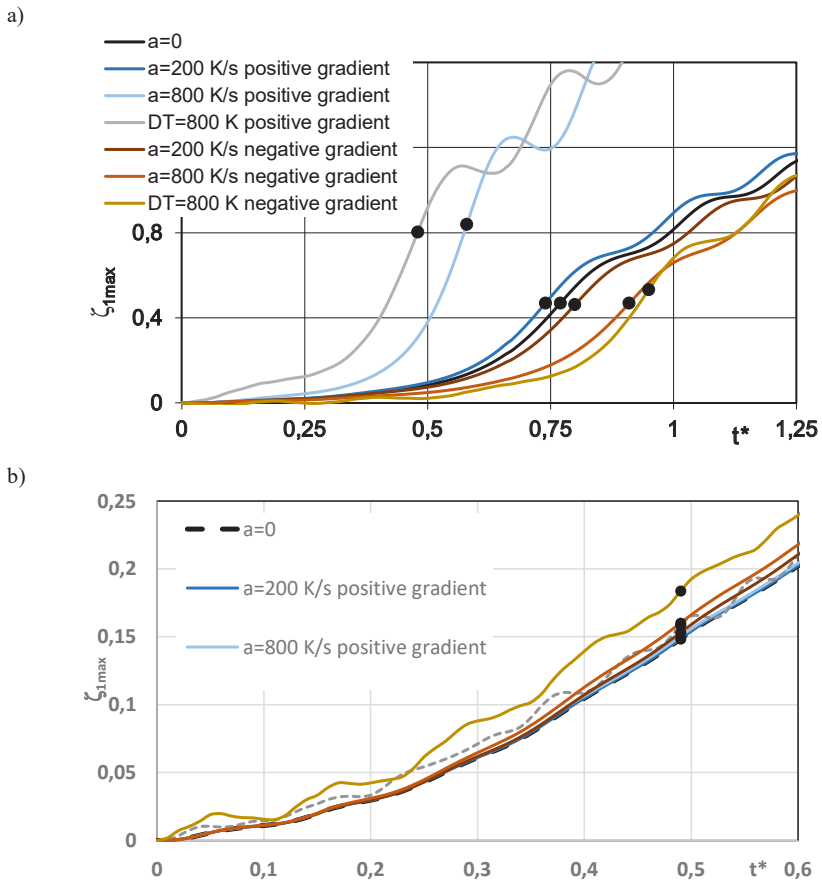

Figure 6: Time histories of deflections for the FDM plate with $\xi_2 = 2$ thermomechanically loaded with various rates a or fixed temperature $\Delta T = 800$ K: a) axisymmetrical plate mode $m = 0$ and b) asymmetrical plate mode $m = 7$.

and increase when the plate is subjected to a negative temperature gradient. Such differences are not observed for the plate mode $m = 7$ (see Fig. 6b). Practically, for all examined cases, the same values of $p_{crdyn} = 22.82$ MPa and the corresponding temperatures $\Delta T_b = 4.9$ K or $\Delta T_b = 19.6$ K for the field characterized by the rate $a = 200$ or 800 K/s, or $\Delta T = 800$ K, respectively, are observed.

Additionally, the effect of the negative value of imperfection ratio ξ_2 has been examined. Selected results are presented in Fig. 7 for the FDM plate model. Plate reactions are for two plate modes $m = 0$ and $m = 7$. The plate is compressed on the outer edge and subjected to an increase in the time–temperature field with a negative gradient. The character of curves $\zeta_{1max} = f(t^*)$ is similar for the examined plate cases. The lack of influence of the negative ratio ξ_2 on the final results is observed. On comparing the results obtained for the asymmetric plate mode $m = 7$ with the axisymmetric one $m = 0$ [11], differences are found in the values of critical parameters: time, deflection, load with the corresponding temperature ΔT_b and also in the supercritical part of curves $\zeta_{1max} = f(t^*)$, where for axisymmetrical plate $m = 0$, the vibrations are initiated.

Figure 8 shows the exemplary results presented for the axisymmetric ($m = 0$) FEM plate model with two imperfection ratios $\xi_2 = 1$ and $\xi_2 = 2$ loaded mechanically and thermally with a temperature difference increasing in time and expressed by a growth parameter $a = 200$ K/s and $a = 800$ K/s. The temperature field has a positive gradient. Time histories of deflections (red lines) and velocity of deflections (blue lines) with critical parameters, time t_{cr} and dynamic load p_{crdyn}, are presented. The nature of the curves is similar. Increase in the temperature difference shortens the time to plate stability loss and decreases the critical dynamic loads p_{crdyn}. This observation is of importance in evaluation of the plate buckling phenomenon.

Additionally, the correspondence of results between the two plate models is shown in Fig. 9. The plate is loaded mechanically and thermally with a positive gradient and a temperature growth rate $a = 200$ K/s. The plate imperfection ratio $\xi_2 = 2$. The lines of time histories of deflections and

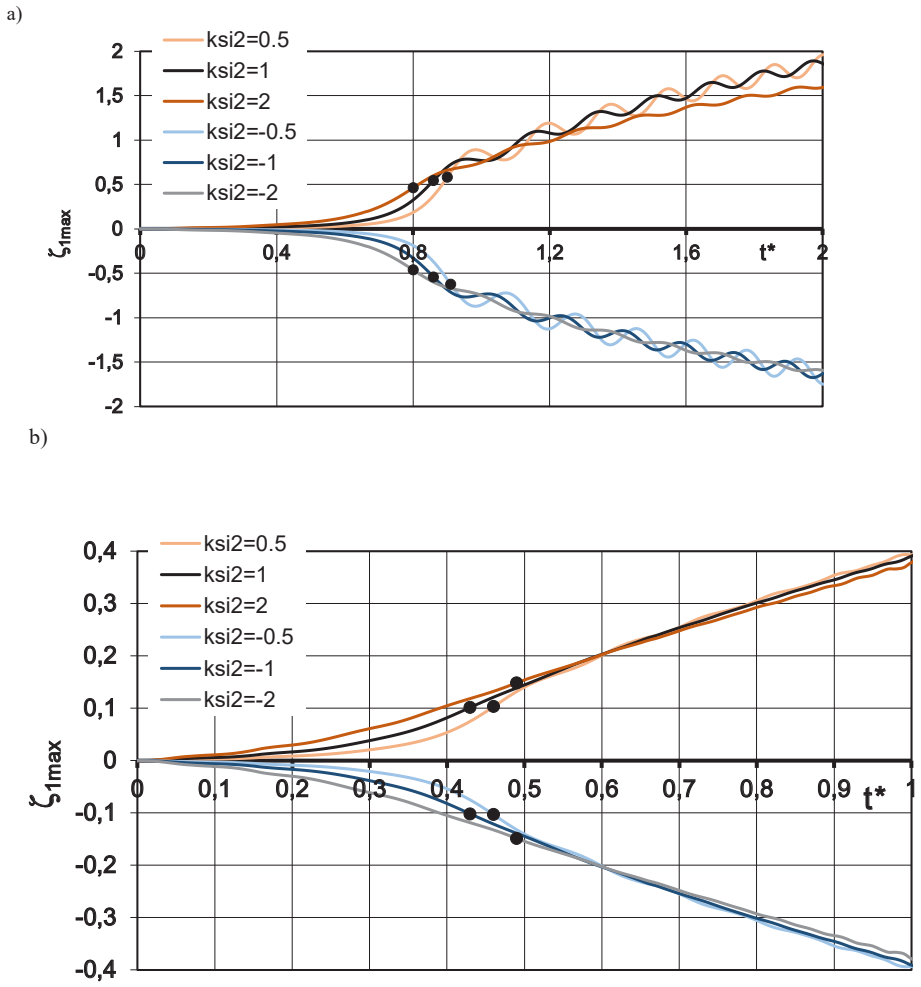

Figure 7: Deflections of a) axisymmetrical plate mode $m = 0$ [11], b) asymmetrical plate mode $m = 7$ versus negative and positive imperfection ratios ξ_2 under mechanical load and thermal load with a negative gradient.

velocity of deflections are similar. The additional black lines indicate the points with a maximum value of the speed of plate deflections. According to the assumed criterion [19], they enable expression of the critical time t_{cr}, critical plate deflection, and, after calculation, dynamic load p_{crdyn} as well as the corresponding difference in temperatures ΔT_b. The presented results are an example confirming the proper calculation process and the method of plate modeling.

The obtained results can be summarized as follows:

- The minimal value of p_{crdyn} which is important in buckling analysis exists for the axisymmetrical $m = 0$ plate model with a greater value of imperfection ratio $\xi_2 = 2$, whose thermal loading is characterized by a positive temperature gradient and a higher value of temperature difference between the plate edges.
- There is a difference between the responses of plates subjected to the temperature field increasing in time and constant in time.
- The direction of temperature gradient affects the values of critical loads p_{crdyn} and the corresponding values of temperature difference ΔT_b. For a positive temperature gradient with an increase in rate a, values of p_{crdyn} decrease and this is the opposite for the negative gradient.
- A greater value of imperfection ratio ξ_2 decreases the critical value of loads: p_{crdyn} and ΔT_b.
- The direction of the plate's initial deflection does not affect the plate response.
- The results obtained for the FDM and FEM plate models are comparable.

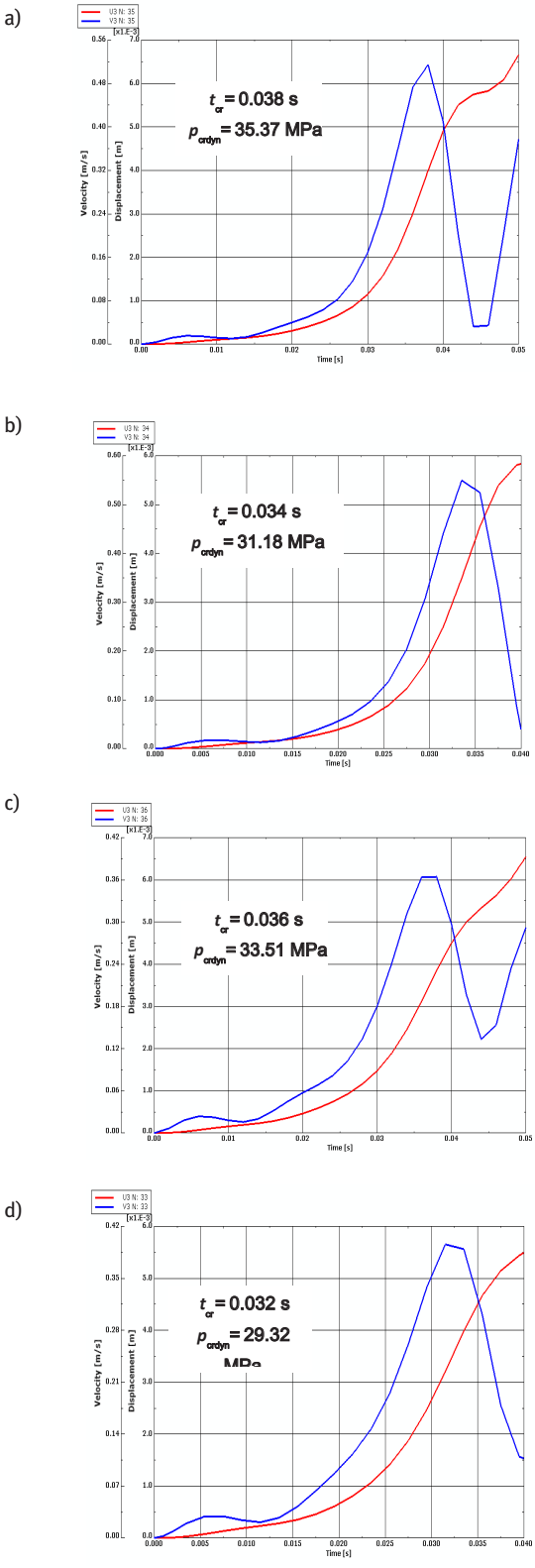

Figure 8: Time histories of deflections and velocity of deflections for the axisymmetrical $m = 0$ FEM plate model thermomechanically loaded with a positive temperature gradient versus different imperfection ratios ξ_2 and temperature growth loads a: a) $\xi_2 = 1$, $a = 200$ K/s, b) $\xi_2 = 1$, $a = 800$ K/s, c) $\xi_2 = 2$, $a = 200$ K/s, d) $\xi_2 = 2$, $a = 800$ K/s.

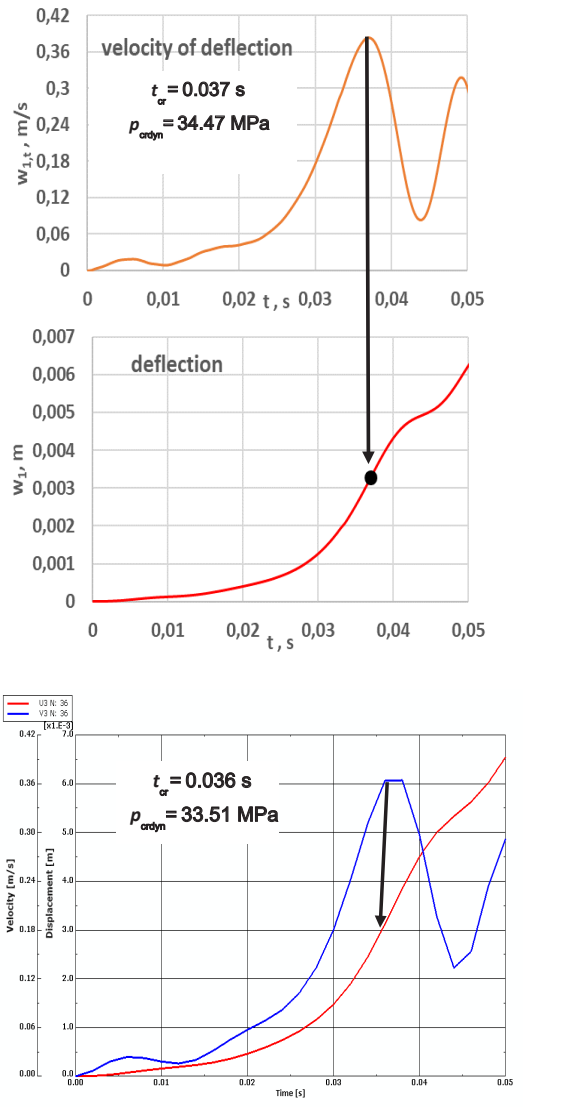

Figure 9: Time histories of deflections and velocity of deflections for a) FDM plate model and b) FEM plate model $m = 0$, $\xi_2 = 1$ loaded mechanically and thermally with a positive temperature gradient and rate $a = 200$ K/s.

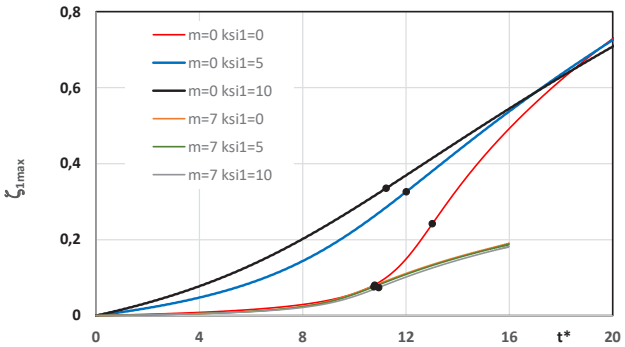

Figure 10: Deflections of the FDM plate model $\xi_2 = 1$ loaded thermally with a positive temperature gradient and rate $a = 200$ K/s versus calibrating number ξ_1.

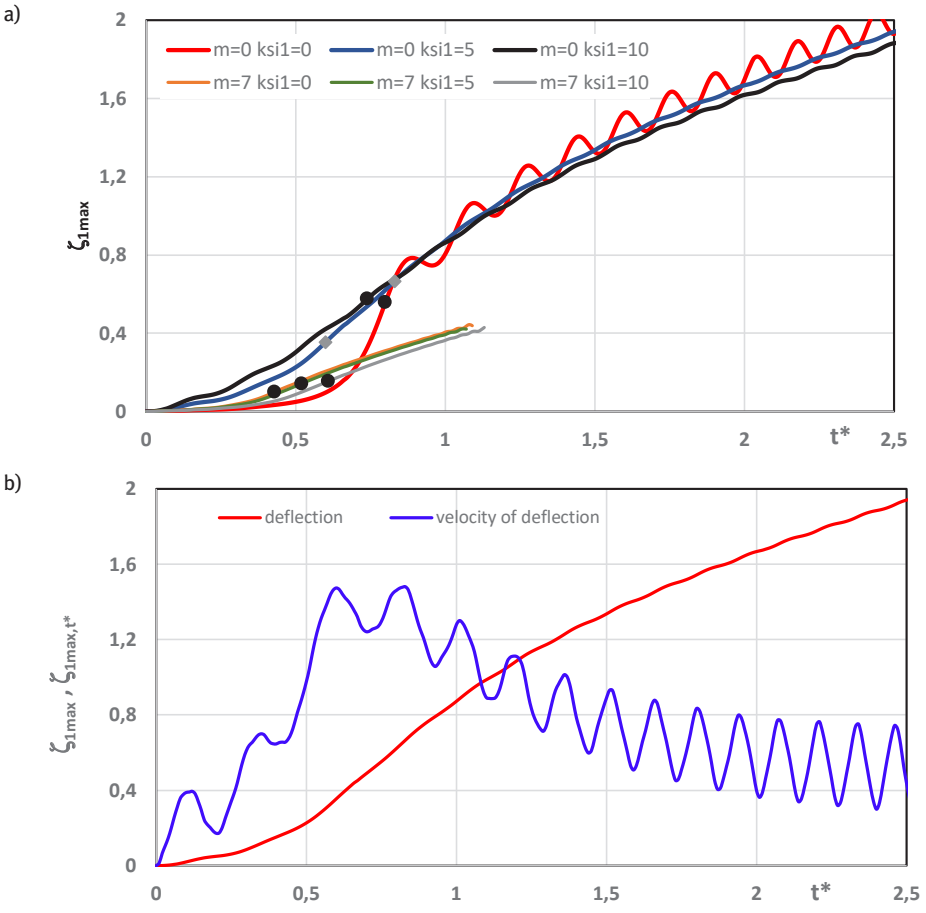

Figure 11: Deflections of the FDM plate model $\xi_2 = 1$ loaded thermomechanically with a positive temperature gradient and rate $a = 200$ K/s versus a) different values of calibrating number ξ_1 and b) value of calibrating number $\xi_1 = 5$ for axisymmetrical plate $m = 0$.

4.4 Plate with a Complex Form of Imperfection

Figures 10 and 11 show the FDM plate model response to thermal and thermomechanical loading. The assumed plate imperfection is composed of two forms: the axisymmetrical one expressed by the calibrating number ξ_1 and the form which is dependent on the number m of circumferential waves $m = 0$ or $m \neq 0$ calibrated by the number ξ_2. Mathematically, this complex form of plate imperfection is described by Equation (9). The form consists of two terms expressed by the aforementioned calibrating numbers ξ_1 (*ksi*1) and ξ_2 (*ksi*2). The plate thermally loaded is subjected to a positive temperature gradient. In the case of complex thermomechanical loading, the plate is mechanically compressed with the forces on the outer edge and subjected to the thermal load with a positive gradient, too. Two exemplary forms of plate buckling are examined: axisymmetrical $m = 0$ and waved with the number $m = 7$ of circumferential buckling waves. The value of the number $\xi_2 = 1$.

Figure 10 shows the plate's behavior which was invoked by thermal loading only. The increase in the axisymmetrical form of imperfection expressed by calibrating the number $\xi_1 = 5$, 10 decreases the values of critical temperature differences by more than 10%. Additionally, critical plate deflections are observed to be increasing. Very small differences in the values of critical parameters exist for the plate with several buckling waves (here, the analyzed number is $m = 7$).

The effect of mechanical loads significantly changes the nature of plate responses. The effect of the additional axisymmetric imperfection shape is presented in Figure 11a. It should be underlined that the main axisymmetrical imperfection is expressed by the second term of Equation (9) for a non-zero value of calibrating number ξ_2. Axisymmetrical ($m = 0$) plates with strong imperfection ($\xi_1 = 10$) lose dynamic stability quicker for smaller values of critical dynamic loads p_{crdyn} and corresponding temperature difference between the plate edges ΔT_b. In the case of the axisymmetrical plate $m = 0$ with the value $\xi_1 = 5$, the area of a possible loss of the plate dynamic stability

a)

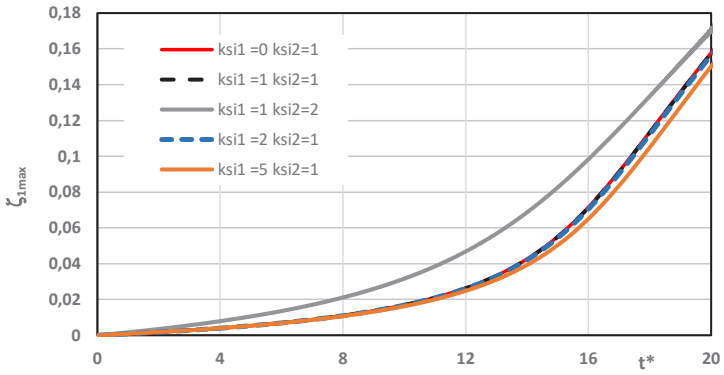

b)

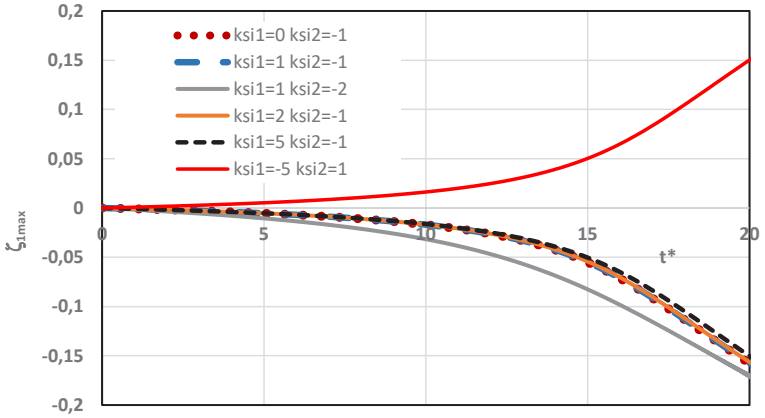

Figure 12: Deflections of the FDM waved $m = 7$ plate model loaded thermally with a positive temperature gradient and rate $a = 200$ K/s for mixed values of imperfection ratios: a) only positive, b) positive and negative.

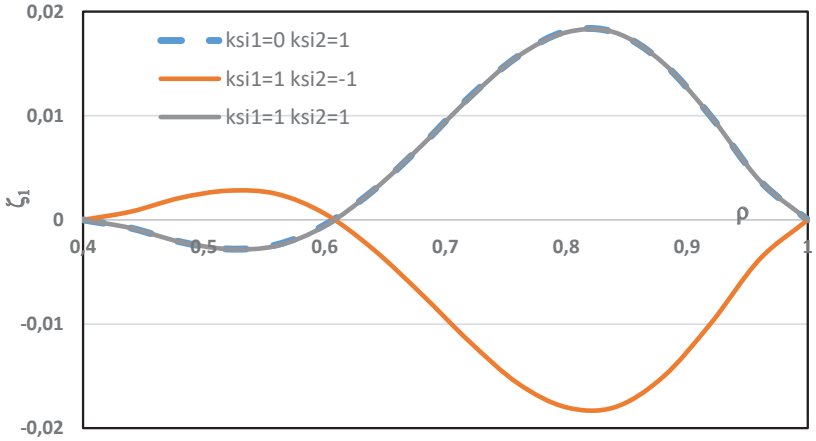

Figure 13: Influence of imperfection ratios on the distribution of the FDM waved $m = 7$ plate model deflections in a radial direction caused by thermal loading with a positive temperature gradient and rate $a = 200$ K/s.

can be expressed, which is between two rectangular gray points shown in Figure 11a. In Figure 11b, the curves of the time history of deflection and time history of the velocity of deflection present the range of the plate stability loss between the points with maximum values of the velocity of deflection. An opposite observation can be made for the waved form of plate buckling ($m = 7$), where the increase in value ξ_1 of additional imperfection shape increases both the values of critical dynamic loads p_{crdyn} and the corresponding temperature ΔT_b. Small fluctuations of critical deflections are observed particularly for the analyzed plate with the number $m = 7$.

The effect of the mixed participation of the values of imperfection ratios on the run of deflection curves $\zeta_{1max} = f(t^*)$ is shown in Figure 12. The results are for the positive numbers of both ratios ξ_1 and ξ_2 or for the positive and negative numbers of ratios ξ_1, ξ_2. The results are presented for the case of the FDM plate model where its form of the loss of stability corresponds to $m = 7$ circumferential waves. The plate is subjected to only thermal loads with a positive gradient. The results show the meaning of the higher positive or negative value of ratio ξ_2, where axisymmetric predeflection also exists ($\xi_1 \neq 0$), and the meaning of the higher values of ratio ξ_1 ($\xi_1 = 5$ or $\xi_1 = -5$) for the positive value of the ratio ξ_2. For assumed values of ξ_1, additional waved shape of predeflection is expressed by the ratio x_2. This complex form of predeflection influences the positive or negative run of plate deflection curve $\zeta_{1max} = f(t^*)$.

The waved form of plate deflection in a radial direction obtained for selected numbers of ratios ξ_1, ξ_2 ($\xi_1 = 0$, $\xi_2 = 1$), ($\xi_1 = 1$, $\xi_2 = 1$), ($\xi_1 = 1$, $\xi_2 = -1$) is shown in Figure 13.

The presented results can be summarized as follows:

- The effect of the additional axisymmetric form of plate predeflection expressed by the calibrating number ξ_1 causes little change to the values of critical temperature differences for the axisymmetrical $m = 0$ form of plate buckling. The increase in the value of calibrating number ξ_1 decreases the value of critical temperature differences.
- The imperfection of plates working in a thermal environment and subjected to mechanical loads has little effect on the critical values, which is dependent on the form of plate buckling.
- The results show that plate dynamic buckling can be expressed by a range of values of critical parameters.
- Values of ratios ξ_1, ξ_2 determining the form of plate predeflection have an effect on plate deflections. The effect of ratio ξ_2 which determines the waved form of plate predeflection is dominant. The participation of the axisymmetrical term of Equation (9) exists for higher values of ξ_1.

5 Conclusions

The paper presents the effect of the temperature field on the stability reaction of a plate with various forms of imperfection. A three-layered annular plate with thin steel facings and a thicker foam core was examined. Different shapes and ratios of imperfection were considered. The thermal effect on the plate response was analyzed for plates subjected to only the thermal environment or plates both mechanically loaded and surrounded by a temperature field that increased in time or was fixed in time. Different elements which characterize the field of assumed loading were taken into account. They are as follows: the temperature gradient direction, the dynamic effect expressed by the rate of temperature difference growth, the effect of the mechanical loading growth, the sensitivity of the examined plate to negative imperfections, and the participation of the axisymmetrical term in complex Equation (9), which expresses the form of imperfection. Vibrations are an additional element which characterizes the dynamic response of the plate. In the undertaken analysis, vibrations were observed in the overcritical region of plate work under the increasing load in time. Particularly, the plate oscillations existed for plates with the axisymmetrical buckling mode $m = 0$ and plates with a small value of predeflection (see Figs 7a and 11a).

The results presented herein show a different effect of imperfection parameters on the values of critical temperature differences for plates located in a temperature field. It depends on the participation of two assumed ratios ξ_1 and ξ_2, which describe the shape of plate predeflection. A rather minimal effect of a single imperfection ratio ξ_2 on the final results has been observed. However, the complicated shape of plate predeflection, which is expressed by the values of imperfection ratios ξ_1 and ξ_2, has an effect on plate thermal dynamic response. Two terms of the plate form of predeflection (see Eq. (9)) calibrated by the ratios, axisymmetrical ξ_1 ($\xi_1 \neq 0$) and waved ξ_2, reveal the plate structure sensitivity. However, the participation of numbers that define plate imperfection is not unambiguous and is difficult to predict in the evaluation of the process of plate buckling behavior. Effective analytical and numerical dynamic analysis is of importance here. The plate reaction to thermomechanical loading depends on many elements, like the parameters of mechanical load, the profile of the temperature field, and dynamic rates of mechanical and thermal growth. The results show the possibility to design the conditions and structure parameters of the composite plate to use it more effectively. Further analyses can

focus on the evaluation of both structural heterogeneities connected with the oriented material properties and the imposed form of plate predeflection to obtain the expected plate reactions on mechanical and thermal loads. Such investigations can be helpful in the plate design process.

References

[1] Chen, Y.R; Chen, L.W.; Wang, C.C. Axisymmetric dynamic instability of rotating polar orthotropic sandwich annular plates with a constrained damping layer. Composite Structures 2006, 73(2), 290-302. doi: 10.1016/j.compstruct.2005.01.039.

[2] Wang, H.J.; Chen, L.W. Axisymmetric dynamic stability of rotating sandwich circular plates. Journal of Vibration and Acoustics 2004, 126, 407-415.

[3] Ghiasian, S.E.; Bagheri, H.; Sadighi, M.; Eslami, M.R. Thermal buckling of shear deformable temperature dependent circular/annular FGM plates, International Journal of Mechanical Sciences 2014, 81, 137-148. http://dx.doi.org/10.1016/j.ijmecsci.2014.02.007.

[4] Kadam, P.A.; Panda, S. Nonlinear analysis of an imperfect radially graded annular plate with a heated edge. Int. J. Mech. Mater. Des. 2014, 10, 281–304. doi:10.1007/s10999-014-9249-y.

[5] Bagheri, H.; Kiani, Y.; Eslami, M.R. Asymmetric thermo-inertial buckling of annular plates, Acta Mech. 2017, 228, 1493-1509. doi:10.1007/s00707-016-1772-5. doi:10.1007/s00707-016-1772-5.

[6] Bagheri, H.; Kiani, Y.; Eslami, M.R. Asymmetric thermal buckling of annular plates on a partial elastic foundation, Journal of Thermal Stresses 2017, 228 40(8), 1015-1029.

[7] Bagheri, H.; Kiani, Y.; Eslami, M.R. Asymmetric thermal buckling of temperature dependent annular FGM plates on a partial elastic foundation, Computers and Mathematics with Applications 2018, 75, 1566-1581.

[8] Zhang, J.; Pan, S.; Chen, L. Dynamic thermal buckling and postbuckling of clamped-clamped imperfect functionally graded annular plates, Nonlinear Dyn. 2019, 95, 565-577.

[9] Shariyat, M.; Behzad, H.; Shaterzadeh, A.R. 3D thermomechanical buckling analysis of perforated annular sector plates with multiaxial material heterogeneities based on curved B-spline elements. Composite Structures 2018, 188, 89-103. https://doi.org/10.1016/j.compstruct.2017.12.065

[10] Alavi, S.H.; Eipakchi, H. Geometry and load effects on transient response of a VFGM annular plate: An analytical approach. Struct. Eng. Mech. 2019, 70(2), 179–197. doi:10.12989/sem.2019.70.2.179.

[11] Pawlus, D. Buckling sensitivity of three-layered annular plates in temperature field on the rate of imperfection. Proceedings of the 8th International Conference on Coupled Instabilities in Metal Structures, Lodz University of Technology, Poland, July 13-15, 2020, cims2020.p.lodz.pl

[12] Pawlus, D. Dynamic stability of three-layered annular plates with wavy forms of buckling. Acta Mech. 2011, 216, 123-138. doi: 10.1007/s00707-010-0352-3

[13] Pawlus, D. Solution to the problem of axisymmetric and asymmetric dynamic instability of three-layered annular plates. Thin-Walled Structures 2011, 49, 660-668. doi: 10.1016/j.tws.2010.09.013.

[14] Pawlus, D. Dynamic stability of three-layered annular plates with viscoelastic core, Scientific Bulletin of the Technical University of Lodz, 1075, Lodz, 2010 (in Polish).

[15] Pawlus, D. Dynamic response of three-layered annular plate with imperfections. Studia Geotechnica et Mechanica 2014, vol. XXXVI, no. 4, 2014, 13-25. doi: 10.2478/seg-2014-0032.

[16] Pawlus, D. Stability of three-layered annular plate in stationary temperature field, Thin-Walled Structures 2019, 144. https://doi.org/10.1016/j.tws.2019.106280.

[17] Pawlus, D. Dynamic response of three-layered annular plates in time-dependent temperature field, International Journal of Structural Stability and Dynamics 2020, Vol. 20, No. 12. doi: 10.1142/S0219455420501394.

[18] Pawlus, D. Dynamic stability of mechanical and thermal loaded three-layered annular plate with viscoelastic core, Vibrations in Physical Systems 2020, Vol. 31, No. 2. https://doi.org/10.21008/j.0860-6897.2020.2.23.

[19] Wolmir, A.S. Nonlinear dynamics of plates and shells. Science, Moscow 1972. (in Russian).

[20] Timoshenko, S.; Goodier, J.N. Theory of Elasticity, Warsaw, Arkady, 1962.

[21] Wojciech, S. Numerical solution of the problem of dynamic stability of annular plates. J. Theor. Appl. Mech. 1979, 17(2), 247–262. (in Polish).

[22] Hibbit, Karlsson & Sorensen, Inc.: ABAQUS/Standard. User's manual. 1998.